A Moored Profiling Instrument*

K. W. DOHERTY, D. E. FRYE, S. P. LIBERATORE, AND J. M. TOOLE

Woods Hole Oceanographic Institution, Woods Hole, Massachusetts

(Manuscript received 13 March 1998, in final form 3 December 1998)

ABSTRACT

The specifications and performance of a moored vertical profiling instrument, designed to acquire near-full-ocean-depth profile time series data at high vertical resolution, are described. The 0.8-m-diameter by 0.4-m-wide device utilizes a traction drive to propel itself along a standard mooring wire at a speed of ~0.3 m s^{-1}. The average power required to profile at this speed is 1–2 W; the present sensor suite and controller draw about 1.5 W. Based on these figures, the instrument's battery capacity will support approximately 1 million meters of profiling. Instrument actions are regulated by an onboard microcontroller, allowing complex dive programs to be carried out. Oceanographic and engineering data are recorded internally on a hard disk interfaced to the controller. The measurement suite thus far deployed includes a CTD for deriving ocean temperature and salinity profiles, and an acoustic current meter that returns ocean velocity profile data. Addition of other oceanographic sensors is anticipated. Results from several trial deployments in the open ocean are reported.

1. Introduction

Society is increasingly concerned with global climate variability. Yet, very few long records of ocean variability that might document secular change currently exist. Time series were once routinely acquired from a network of ocean weather ships, and these data provide a tantalizing glimpse of ocean variability on seasonal to decadal timescales (e.g., Lazier 1980; Østerhus et al. 1996; Talley and Raymer 1982; Talley 1996; Joyce and Robbins 1996; Karl and Michaels 1996; Denman et al. 1992; Freeland et al. 1997). However, the logistics and costs of using ships to maintain such stations has become prohibitive. Only a handful of sites are presently sampled, some at rather long and irregular time intervals. Here a moored instrument (termed the Moored Profiler) capable of autonomous, near-full-water-column profiling is described. This device, when deployed in combination with drifting, gliding, and/or self-propelled profiling vehicles, shows promise for effectively monitoring future climatic ocean change. The new instrument is also well suited for short-term, process-oriented experiments that require information at high-vertical and temporal resolution.

Ocean time series data are routinely collected using moorings with discrete instrumentation. The ATLAS buoys presently forming an array in the equatorial Pacific Ocean, for example, utilize a set of individual temperature sensors spanning the upper 500 m of the water column (Hayes et al. 1991). In similar fashion, surface moorings with discrete physical and biological oceanographic sensors are being maintained at stations offshore from Bermuda and Hawaii, respectively, supplementing ship-based observation programs (Dickey et al. 1997; R. Lukas 1997, personal communication). A major difficulty with this multiple-sensor approach, beyond the expense, is the determination of relative sensor calibrations. For example, discrimination between a truly well mixed layer, and one with residual stratification can be ambiguous if individual sensors have unknown offsets. This is a particular problem for conductivity sensors that are prone to calibration drift. Profiling instrumentation in which one instrument package moves vertically through the water column significantly reduces this uncertainty.

Moored profiling systems have been utilized in the past to obtain upper-ocean time series information. The Cyclesonde (van Leer et al. 1974) and the Profiling Current Meter (PCM; Eriksen et al. 1982) employ variable buoyancy to move vertically over a limited depth range. More recently, Provost and du Chaffaut (1996) have developed a buoyancy-driven profiler capable of cycling to 1000-m depth. In contrast, Eckert et al. (1989) describe a profiling instrument platform that derives vertical lift from ambient currents, and Fowler et al. (1997) have devised a method to extract energy for profiling from surface-wave-induced mooring motion. Distinct

* Woods Hole Oceanographic Institution Contribution Number 9696.

Corresponding author address: Dr. J. M. Toole, WHOI, Clark MS #21, Woods Hole, MA 02543.
E-mail: jtoole@whoi.edu

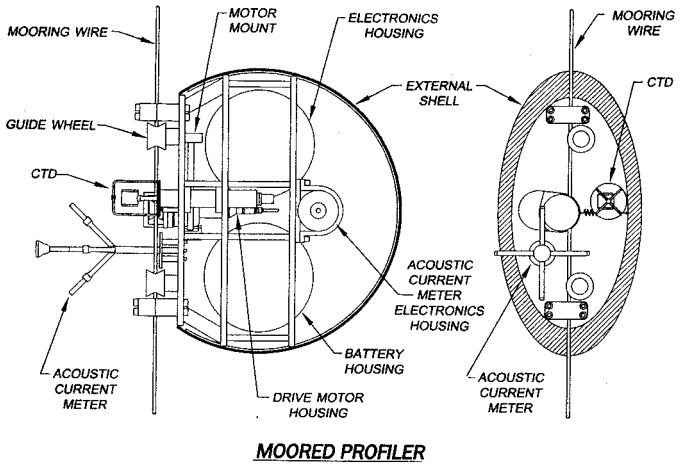

FIG. 1. A schematic drawing of the Moored Profiler equipped with a CTD and acoustic current meter.

from these techniques, the system described here uses a motorized traction drive to propel itself vertically. The general specifications for the new instrument are discussed below. Section 2 details the mechanical design of the profiler and its control system. Results from trial deployments in the open ocean are given in section 3.

The basic design of the new system was defined through specification of its scientific requirements. The ability to profile over the full water column, from within the surface mixed layer to within about 100 m of the ocean bottom, was stipulated. This sampling range allows the exploration of relationships between upper-ocean changes and those at depth. Furthermore, decomposition of ocean variability in terms of vertical modes is facilitated with full-depth information (e.g., Hayes et al. 1985). From a practical standpoint, deep profiles can provide in situ checks of sensor calibrations by sampling water properties at levels known to be stable on annual timescales. Cycling to great depth (and positioning the instrument at depth between cycles) additionally improves data quality (sensor stability) by inhibiting biofouling. To minimize mooring motion and thereby facilitate deployments of a year or longer, a subsurface mooring configuration was chosen. With care, subsurface moorings can be deployed to within 25 m of the surface. It is recognized, however, that mooring blowdown by strong currents might at times limit access to very shallow mixed layers.

Flexible temporal sampling was specified to address diverse scientific problems. For climate monitoring studies, our goal was to obtain better than monthly resolution in analyzed data from a 1-yr deployment, thereby resolving the seasonal cycle, including any embedded changes on 1–2-week periods. For design purposes, a mission was defined as 100 round-trips to 5000 m, yielding 200 full-depth vertical profiles, or about 1 million meters of vertical travel, per deployment. It was recognized that users of the new instrument might wish to highlight one depth interval over another, or to focus attention on one or more time periods in the year. To accommodate this, the profiler was designed to allow variable depth sampling based on a user-defined sampling schedule. For example, deployments focusing on internal wave variability have been made where instruments profiled every 1 to 2 h over about a 1-km segment of the water column for 1-month intervals. Alternatively, an instrument set to observe winter convection might be programmed to acquire several profiles a day in midwinter, dropping back to only a few samples per week in the other seasons.

Energy considerations, and concern with aliasing, set bounds on profiling speed. High speed incurs excessive energy dissipation through hydrodynamic drag. Slow speed can introduce spurious vertical structure in profiles when depth segments are sampled at different tidal phases. The compromise speed of 0.3 m s^{-1} was chosen (which is near optimal from an energetic standpoint, see below); at this rate a 5000-m profile is collected over a time span of approximately 4.6 h. An individual, full-depth profile is thus subject to some tidal aliasing. Burst sampling (e.g., collecting five profiles within a one-day period every fifth day as opposed to doing one profile each day) is one technique to combat these errors.

The chief design issue for the new instrument was the mechanism to propel it vertically. As noted above, several ocean profilers developed previously employed variable displacement devices; others relied on ambient flow or mooring motion. In contrast, the new instrument utilizes an electrical motor, gear train, and traction wheel to move itself along the mooring wire. Conceptually this approach was attractive since it takes advantage of the existence of the mooring wire, allows maximum profiling flexibility, and is relatively inexpensive to implement. Reliance on lift from ambient currents or mooring motion over the full water column was deemed uncertain, especially in the deep ocean where currents may be low for long periods of time and mooring motion is reduced. From an energy standpoint, there is little to separate buoyancy-change devices from traction systems in a moored configuration. Both expend battery energy in doing work to move verticlly, and both suffer inefficiencies through electromechanical system losses and hydrodynamic drag. Our design study found that the requirement for a full-ocean-depth operating range presented complications in using a variable displacement system because of the large pressure forces that are incurred at great depth. Furthermore, a traction drive appeared capable of carrying out complex sampling scenarios (repeated shallow cycles interspersed with full-depth sampling for instance) and was able to apply additional force to pass obstructions on the wire in a more energy efficient manner than could a variable-buoyancy system.

Last, the vehicle was envisaged supporting a diverse set of oceanographic instrumentation. It was accepted that all systems would include a conductivity–temperature–depth (CTD) instrument for observing finescale temperature and salinity information as a function of

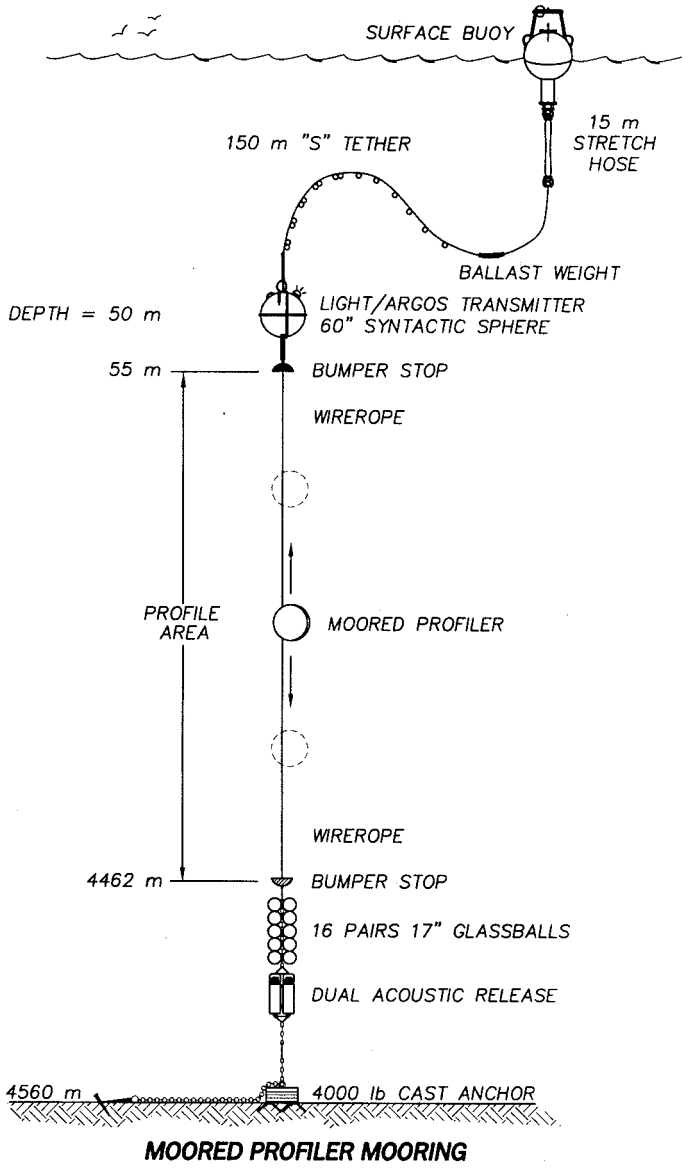

FIG. 2. A representative mooring diagram for a profiler equipped with a real-time telemetry link.

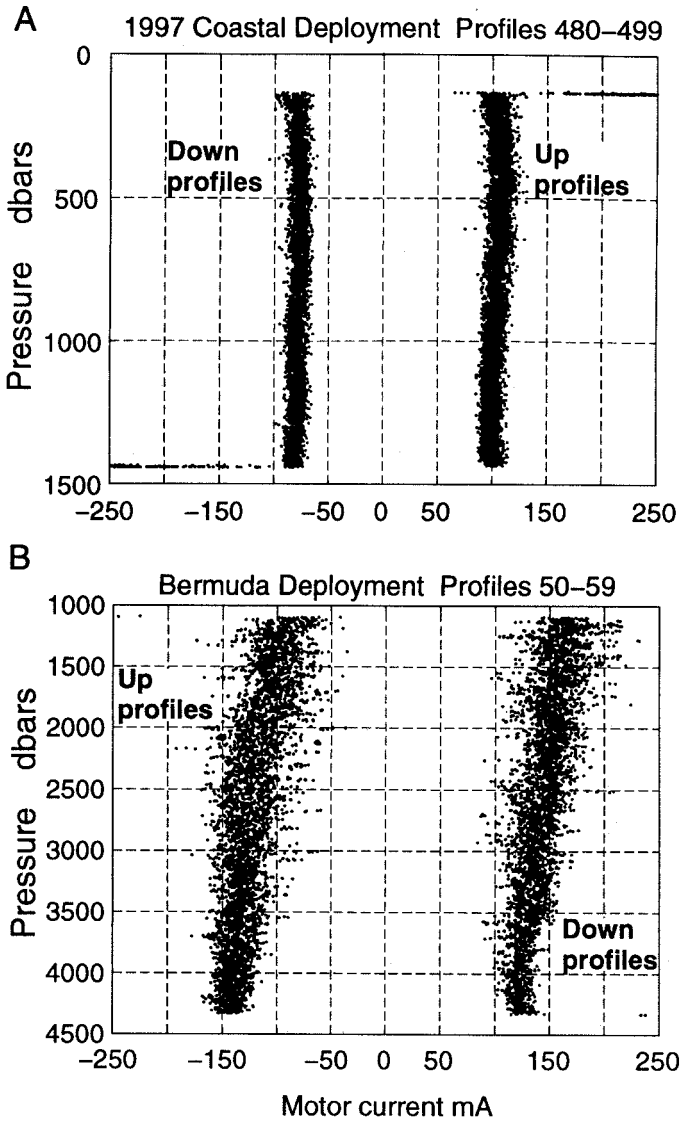

FIG. 3. Instantaneous estimates (300-ms averages recorded every 11 s) of motor current as a function of profiler depth from (a) the fall 1997 profiler deployment on the continental slope south of New England and (b) offshore from Bermuda in spring 1997. Up-going profiles are displayed with positive motor current values, down-going with negative values. Large-magnitude motor currents are observed when the instrument impacts the mooring stops at the top and bottom.

pressure. Provision for easy addition of other sensors constituted a major design element for the system electronics. Our design assumes that each sensor maintains an accurate time base during a profile so that pressure data from the CTD may be used to register these other observations in depth.

2. Instrument design

A prototype of the Moored Profiler was constructed and tested in the Woods Hole Oceanographic Institution (WHOI) tow-tank facility, and at the WHOI dock. Based on this work, ocean-going systems were developed and deployed for testing on deep-sea moorings. Second-generation instruments were subsequently developed to address shortcomings in the initial design revealed during sea trials. The current version of the instrument system is described here.

The Moored Profiler consists of a propulsion system, controller, sensor suite, batteries, and buoyancy elements, housed within a segmented oblate–spheroidal cowling of vacuum-bagged polyester fiberglass (Fig. 1). The instrument is deployed on a conventional plastic-jacketed wire rope in an oceanographic mooring (Fig. 2) and repeatedly traverses that length based on a user-defined operation program. The profiler's cowling has a 2:1 aspect ratio with a major-axis diameter of 0.8 m. This basic shape was selected for low drag (C_d is approximately 0.16, Savage and Hersey 1968), and symmetry with respect to horizontal and vertical flows. The mooring wire threads vertically through the leading edge of the instrument, guided by sheaves at the upper and lower ends of the front surface. The sheaves, whose

axles are oriented fore–aft, have a broad V-shaped bearing surface with diameter decreasing from 7.62 cm at the ends to 5.08 cm in the center. Torlon® ball bearings are used with bearing races and wheels manufactured from acetron® NS, a filled acetal plastic having excellent wear characteristics. Location of the mooring wire near the leading edge of the instrument allows the body to align with the horizontal flow. This minimizes drag forces caused by horizontal currents and positions the oceanographic sensors in undisturbed flow. Retaining brackets at each sheave, used to constrain the instrument on the mooring wire, support the weight of the profiler on deployment and recovery when the mooring wire is horizontal. These have a cross-sectional clearance of 19.6 cm^2, allowing the instrument to pass over obstructions on the mooring wire.

The propulsion unit is mounted on a hinge that allows the drive wheel to pass over obstructions on the mooring wire. The drive wheel is a 4.4-cm-diameter sheave positioned between the guide sheaves in the same fore–aft orientation. This arrangement negates the need for a right-angle gear in the drive train (with its attendant losses). A high-friction coating is applied to the surface of the wheel to minimize slippage. The wheel is held against the mooring wire by a spring that exerts a tension of 35.6 N in normal operation. This tension in turn acts to center the wire on the drive and guide sheaves. The heart of the propulsion system is a brush-type DC motor from Maxon Precision Motors, Inc., running in air at approximately 3500 rpm through a 27-to-1 gear. The motor is specified by the manufacturer to be 84% efficient, while the gear train is rated at 75%, giving a total electrical to mechanical conversion efficiency of 63%. A magnetic coupler is used to transfer motor torque across the titanium motor housing to the drive wheel. The coupler is capable of delivering 0.5 N m of torque. Thus, the maximum driving force that can be applied to the profiler is 22.7 N. In normal operation, the motor turns the drive wheel at approximately 130 rpm to give the profiler ascent/descent rates of approximately 0.3 m s^{-1}. The direction of travel is determined by the sense of the voltage applied to the motor. A dynamic brake was created using a switch that shunts the motor leads to ground. The induced electromotive force (emf) developed if the drive wheel is rotated when the switch is closed, acts to resist profiler motion.

Profile speed was chosen in light of the efficiency curve for the Moored Profiler. Mathematically, this begins with an energy equation of the form $ED^{-1} = F_D e^{-1} + Hw^{-1}$, where E is the energy expended on one profile of length D, F_D represents the drag force (typically modeled as a squared velocity law), e is the efficiency of the motor and drive train, H is the (constant) electrical power drawn by the instrumentation and controller (the "hotel" load), and w is the profile speed. This relation may be used to predict the optimal profile speed between fast travel, where drag losses become prohibitive, and slow travel, where the hotel load is limiting. With $F_D = \rho C_d A w^2$ and ignoring variations in e, the optimal speed is given as $w_{optimum} = [eH/(2\rho C_d A)]^{1/3}$. For the Moored Profiler fitted with a CTD and ACM, the hotel load is ~1.5 W giving $w_{optimum} \sim 0.2$ m s^{-1}. But tidal aliasing concerns become more severe at slow profile speed. As the efficiency curve is quite flat about the optimum speed, we opted for a somewhat faster-than-optimal profile speed of 0.3 m s^{-1} at the cost of using ~15% more energy per profile.

The internal frame holding the various profiler components is machined from ultrahigh molecular weight polyethylene, which is slightly buoyant in seawater. The internal components include two 0.30-m-diameter glass balls that provide pressure vessels for the instrument electronics and batteries, as well as buoyancy for the device. Power for the various systems is supplied by two lithium battery packs (combined mass of 7.3 kg) assembled from double-D-format cells that are mounted in the lower of the two glass balls. The pack supplying the drive system has an open-circuit voltage of 14.4 V and a 150 A h capacity, that supporting the scientific instrumentation is specified at 10.8 V and 120 A h. Underwater cables between the various pressure vessels distribute electrical power, and support system-control communications and data transfers. A titanium strain-gauge pressure sensor mounted on the electronics sphere and sampled by the instrument controller is used to monitor instrument depth. (A dedicated sensor was employed to simplify development; in future, pressure information will be obtained from the CTD instrument.)

Profiler operations are regulated by a low-power (<0.02 W average consumption during profiling) microcontroller manufactured by Onset Computers, Inc. (This value and subsequent power estimates for the instrumentation are based on a supply voltage of 10.5 V.) Operationally, the profiler travels between a series of user-defined depth stations, with variable wait-periods between each cycle. For example, an instrument might be programmed to rapidly cycle 10 times over the upper 1 km of the water column, perform a full-depth profile, then wait three days before repeating the pattern. Limited problem solving has also been implemented to overcome obstructions on the wire. If vertical travel is blocked, the profiler can be instructed to back up and try again to move through the problem spot. If after several tries it cannot pass the obstruction, the instrument reverses direction and proceeds to its next depth station. The microcontroller also monitors the battery levels and terminates operations if the voltage of either pack falls below user-specified levels (typically three-quarters of their initial open-circuit voltages). This action reduces the chance of venting that can occur when batteries are fully drained. The voltage test is based on average values over several hours of profiler operation. Thus, single spurious voltage values will not prematurely terminate operations.

Moored Profilers constructed to date have been equipped with CTD instruments manufactured by Fal-

mouth Scientific, Inc. (FSI, their Micro-CTD™). This instrument was chosen for its small size (36 cm in length, 5 cm in diameter), relatively low power consumption (1.2 W; a new version of the instrument is in development that will consume 10% of the power of the present version), and freely flushing sensors. The manufacturer's specifications for the accuracy of the pressure, temperature, and conductivity sensors of this instrument are ±5 db, ±0.005°C, and ±0.0005 S m^{-1}, respectively. The CTD is mounted through the forward plate of the profiler body with the sensors extending out approximately 10 cm. The instrument is supplied with 1 Mbyte of internal RAM for temporary data storage during profile operations. The CTDs deployed to date have sampled at 1.65 Hz. Several Moored Profilers have also been equipped with an FSI 3D-ACM™ acoustic phase-shift current meter with a customized, remotely mounted sensor head. The ACM consumes less than 0.3 W of power. The remote mounting allows for the electronics pressure case to be housed fully inside the profiler cowling. The horizontal arrangement of the case required a special mount for the standard tilt sensors; no change was required to the three-axis compass. The standard ACM "sting" was modified to the 45° pyramid arrangement seen in Fig. 1 to minimize measurement errors caused by wakes off the struts supporting the acoustic transducers. Tow-tank tests were conducted to verify the performance of the modified design. As the profiler is free to align with the horizontal flow, the modified arrangement presents two orthogonal horizontal acoustic paths and one vertically angled path to the incident flow that are upstream of any wake-generating support struts. As with the CTD, the raw data from the ACM (four path–velocity values, three components of magnetic compass and two of tilt, all logged at 2 Hz) are temporarily recorded on internal RAM during each profile. Communications between the instrument controller and external oceanographic sensors follow the RS-485 standard.

The mass of an assembled profiler, depending on instrumentation, is 42–49 kg. In operation, the instruments are typically ballasted to be neutrally buoyant at middepth. The use of plastics and glass enhance the system's compressibility, thereby minimizing buoyancy forces incurred during profiling. Mechanical adjustment of the profiler displacement during a depth cycle is not required as the maximum buoyancy forces experienced during a 5000-m profile are less than 2.5 N. Furthermore, this buoyancy change causes minimal energy loss since work against gravity in one direction of profiling is returned in the other direction. Ballasting (carried out shoreside following standard procedures) involves weighing the assembled instrument in air and in a water bath of known temperature and density. The mass adjustment to achieve neutral buoyancy at midocean depth is derived using estimates of the instrument's effective compressibility and thermal expansion coefficient and a representative in situ ocean temperature and density profile from the deployment site. Based on the efficiency curve of the drive motor, we estimate that the overall system efficiency is little changed by ballasting errors as large as 0.4 kg because the added power required to move in one direction is largely compensated by reduced power in the other. However, drive wheel traction must also be considered; gross misballasting will result in wheel slip. Increasing the drive-wheel spring tension can reduce the chance of slipping, but at the expense of more rolling friction and wear. As presently configured, we judge the instrument able to tolerate ballasting errors up to about 0.15 kg without significant change in performance.

Vertical travel of the instrument along the mooring line is regulated by the controller, based on the observed pressure. At the start of a profile, the CTD and ACM are powered up and instructed to acquire and store their respective raw data. Engineering data (pressure, battery voltages, and electrical current to the drive motor) are acquired independently by the controller at 0.091 Hz and are also temporarily stored. A profile continues until the instrument achieves a scheduled pressure level, or an obstruction blocks travel along the cable. Rate of travel is estimated over a user-specified time interval (typically 1–3 min) from the time-rate-of-change of observed pressure. The system concludes that it is stalled when the average travel speed falls below a preset value, typically 10 cm s^{-1}.

Upon completion of a vertical profile, the CTD and ACM sampling is halted. The CTD data are then downloaded to the controller's RAM, combined with the engineering data, and archived to the hard disk interfaced to the controller. Data are written to disk in ½-Mbyte blocks. (Fixed block size is a limitation of the Onset controller.) In normal operation, the CTD and engineering data acquired during a 5000-m profile fill ~60% of a block. ACM data are subsequently offloaded and archived, again in ½-Mbyte blocks. (Two to three blocks are required for a 5000-m profile.) It takes approximately 10 min to transfer each block of data to the controller and about 10 s to write these data to disk. (Each disk write, including the 3-s period when the disk is accelerated to speed, consumes ~34 J, a negligible part of the overall energy budget.) Then, depending on the operation program, the instrument either proceeds to its next depth station or enters a "sleep" mode for a user-specified period. In the case of short profiles, multiple data segments are logged in the FSI instrument RAMs prior to disk archiving (thereby optimizing disk storage space). Profile segments are separated in the data files by two full data scans holding null values for each variable. Time is recorded at the initiation of each data collection cycle. These times, plus the respective sample rates of the CTD, ACM, and engineering data, are used to derive the time of each datum. Pressure data from the CTD are then used to register each observation in depth.

To facilitate, monitoring instrument performance

from a support vessel (e.g., to verify operation after deployment), the profiler has been fitted with an acoustic transponder. Operationally, the vessel holds position over the mooring and a series of acoustic ranges are taken over a 5–10-min interval (using a standard acoustic release deck unit). A single range value is usually sufficient to roughly determine where the profiler is along the mooring wire. Variation of range with time denotes profiler motion (assuming station keeping is reasonably good). In addition to this simple system, a real-time data telemetry link has been designed and dock tested but not as yet demonstrated at sea.

System installations to date have followed standard "anchor-last" deployment procedures. Typically, the profiler is attached to the mooring wire after the main buoyancy and a few hundred meters of mooring wire have been trailed overboard. A slip line is used to ease the instrument into the water. Drag on the profiler during the subsequent pay-out of the remaining wire pushes the instrument up against the top mooring stop (placed to prevent profiler impact with the wire termination) so no major impact shock occurs when the anchor is released. Overvoltage circuitry protects the profiler electronics from induced emf caused by drive-wheel-induced motor turning during deployment. Standard recovery procedures are also followed, though some skill is required with short (~1000 m) moorings to quickly initiate the tow on the mooring line so that the backup buoyancy stays clear of the profiler after release. Serial firing of two releases spanning the backup buoyancy, or doing without back-up buoyancy, has also proven effective for short moorings.

3. Instrument performance

Observations gathered during several ocean deployments will be used to highlight the performance of the Moored Profiler. A coastal deployment of an instrument equipped with both a CTD and an ACM was made near the 1500-m isobath south of Woods Hole in September–October 1997. The mooring consisted of a 1.22-m-diameter steel buoyancy sphere positioned at ~90-m depth (providing 5938 N of buoyancy), a single 1300-m length of 0.64-cm-diameter jacketed wire rope, dual releases in series spanning backup buoyancy (glass balls), 20 m of 2.5-cm plaited nylon rope and a 1360-kg cast-iron anchor. The Moored Profiler was programmed to cycle continuously in time between stops on the wire at ~100- and ~1400-m depth, pausing only as long as it took to archive data from the CTD and ACM to hard disk. The instrument completed 501 vertical profiles between 100- and 1400-m depth during the 36-day deployment and was attempting profile number 502 when the release was fired and the mooring recovered. Total vertical distance profiled on this trial was 652 000 m; analysis of the drive-system battery after recovery suggested that it was on schedule to meet the design goal of one million meters. The only irregularity in the profiling was a 4-h interruption caused by a communication error between the controller and the oceanographic sensors. The controller software failed to deal with this error in a timely fashion but was eventually able to resume regular profiling. (Controller software has since been revised to increase the profiler's reliability.)

Deep-ocean performance is described using data from an older-style profiler fitted with a CTD deployed in 4500 m of water southeast of Bermuda in June–July 1997. This version of the profiler had the guide and drive wheels enclosed inside the instrument cowling, and had minimal clearance for the mooring wire at the guide wheels. It was, consequently, prone to fouling. The mooring consisted of a 1.52-m-diameter syntactic foam buoyancy sphere (providing 3923 N of buoyancy), a single 4400-m length of 0.64-cm-diameter jacketed wire rope, back-up buoyancy, a release, and a 1800-kg cast-iron anchor. Once deployed, the top wire stop was located at 60-m depth. However, an unknown agent fouled this instrument during the deployment operation. The profiler eventually freed itself, but the fouling material effectively acted as a top stop at ~1300 m during this trial. This instrument was programmed to pause for 24 h at the bottom stop between profiles, but only long enough to archive data at the top stop. This instrument completed 60 profiles between 4300 and ~1300 m before it was recovered.

a. Mechanical system

Our principal diagnostic for the propulsion system is the motor current, sampled every 11 s during profiling. During the fall 1997 coastal deployment, motor current varied between about 80 and 120 mA from the unregulated 14-V supply, which translates to a power expenditure of 1.1–1.7 W (Fig. 3a). The hydrodynamic drag (based on a speed of 0.3 m s^{-1}, 0.25 m^2 cross-sectional area, and drag coefficient of 0.16) accounts for roughly half of the power expended, as expected from the manufacturer's quoted motor and drive-train efficiency. Somewhat greater current was drawn during these up-profiles than down-profiles (Fig. 3a), suggesting that the profiler had been ballasted heavy. Based on the up–down motor current difference and the relationship between motor current and torque, we estimate that this instrument carried 70 gm of excess ballast weight. Profile-averaged motor current varied during the deployment (Fig. 4a). Initially, both up- and down-profile average current fell with time, possibly because frictional losses were reduced as drive-train components and guide wheels were broken in. Subsequent variations appear related to profile speed (Fig. 4b) which, in turn, is a function of the incident currents (Fig. 4d). This association with ambient currents is seen more clearly in total energy expended on each profile (Fig. 4c). We surmise that stronger horizontal currents cause higher drag forces on the profiler body that increase the loads on the guide and drive wheel bearings and ultimately,

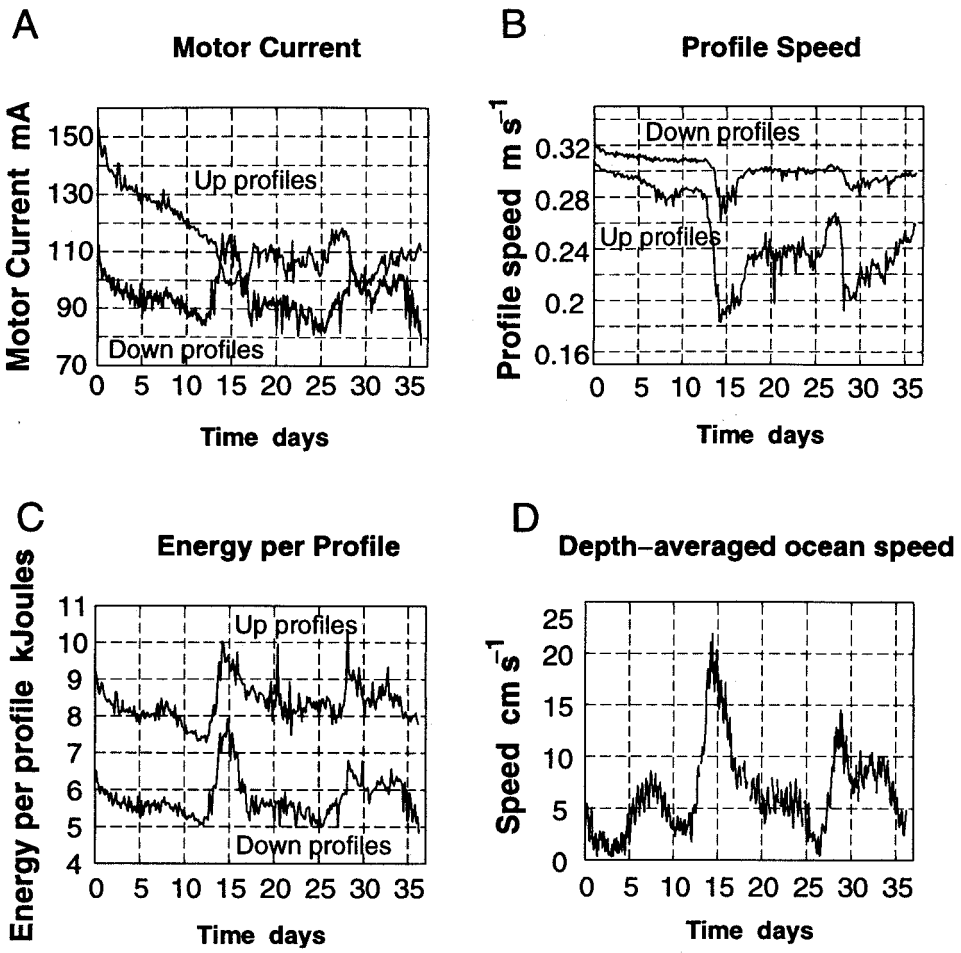

FIG. 4. Engineering data from the fall 1997 profiler deployment on the continental slope south of New England. (a) Profile-averaged motor current versus time for the up-going (light line) and down-going (bold line) profiles. (b) Profile-averaged speed versus time for the up-going and down-going profiles. Down-profiles were faster than up-profiles. (c) Total energy expended by the drive system per vertical profile. Down-profiles took less energy than up-profiles. (d) Depth-averaged (100–300 m) horizontal ocean current speed vs time derived from the data acquired by the acoustic current meter fitted to the Moored Profiler.

their frictional losses. Additional energy is thus required to profile, and profile speed is somewhat diminished. But slower profile speed reduces hydrodynamic drag losses, which partially compensates in the total energy expenditure per profile. The deployment-averaged energy expenditure for vertical profiling during this trial was 5.7 J m^{-1}. This figure extrapolates to 1583 W h to profile 1 million meters; the battery for the propulsion system is rated at about 2100 W h.

Comparable drive system performance was seen in the deep-ocean deployments off Bermuda. Motor current ranged between 100 and 200 mA with somewhat greater scatter than seen during the coastal deployment (Fig. 3b). Motor current noise is caused by fluctuations in drive-wheel speed. The enhanced variability suggests the profiler experienced larger-amplitude vertical wire motions on the 4500-m Bermuda mooring than on the 1500-m coastal mooring, as might be expected from consideration of wire stretch. Up- and down-profile motor current values were comparable at about 3500-m depth during the Bermuda deployment, suggesting that this instrument had been ballasted well. The greater span of ocean in situ density and incurred buoyancy forces on this deployment, as compared to the coastal deployment, is reflected in a slightly larger top-to-bottom range in motor current. The top-to-bottom range is not large, however ($\lesssim$50 mA); this behavior convinced us that neither active nor dedicated passive ballast control (beyond choice of construction materials) was necessary. Indeed, the average energy expended to profile during this deployment was 7.1 J m^{-1}, which is close to the figure obtained on the coastal deployment.

Compass and velocity data from the ACM acquired during the coastal trial shed light on the azimuthal behavior of the profiler. At incident horizontal-current speeds less than about 10 cm s^{-1}, the profiler appears to align closely with the incident horizontal flow. The orientation of the instrument in geographic coordinates thus varies slowly with time (depth) depending on the structure of the horizontal flow (Fig. 5a). In stronger

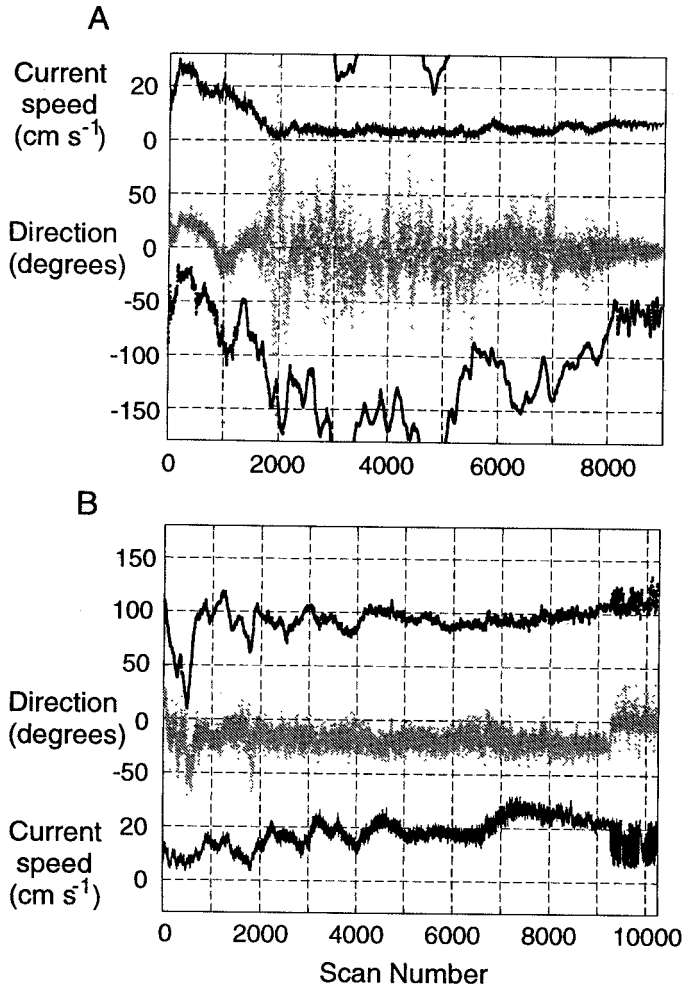

FIG. 5. Time series (at 2-Hz sampling) of the profiler compass heading (black dots) and the relative direction (gray dots) and speed (thin line) of the measured horizontal currents relative to the instrument for two down-going profiles. (a) Time of weak horizontal ocean flow and (b) during stronger flow. Alignment of the incident horizontal flow with the profiler corresponds to a relative direction of 0°. A profiler compass heading of 0° indicates the body pointing eastward. Note the wagging seen in the instrument heading and its signature in the measured horizontal current in (b) after stop impact at scan ~9200.

currents, the instrument appears to adopt a persistent angle to the incident flow of about 20°, independent of profile direction, possibly due to asymmetries in the cowling and/or sensor arrangement (Fig. 5b). This attitude presents greater surface area to the horizontal flow and likely increases drag somewhat. The incident angle of the relative flow at these times does remain within the valid measurement sector of the ACM, however. After impacting the mooring stops, the profiler frequently oscillates through ±15° at a period of 10–20 s; signature of this wagging is evident in the velocity data after about scan 9500 in Fig. 5b. We may be seeing the effects of vortex shedding off the instrument cowling, though it is unclear why this happens only when the instrument is at rest. A tail fin to improve the profiler's alignment with the flow and reduce its wagging has been considered but not yet implemented.

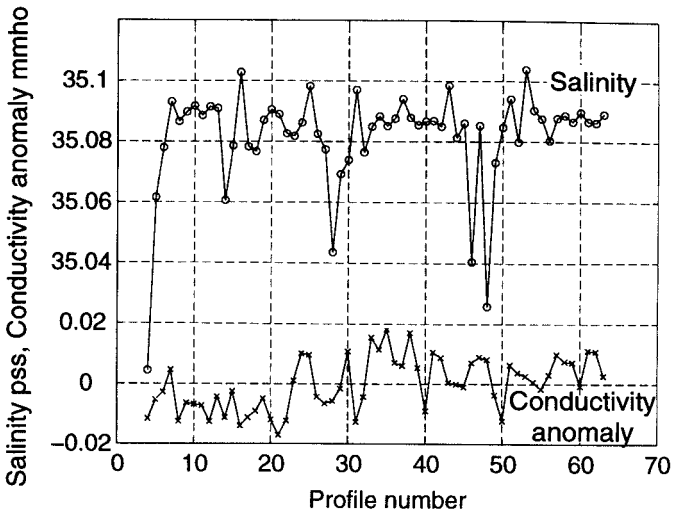

FIG. 6. Variation of observed conductivity averaged between potential temperature 2.25° and 2.75°C as a function of profile number for the 1997 Bermuda deployment (×). Also shown is the variation of salinity averaged between potential temperature 5.0° and 5.5°C in the main thermocline after a profile-dependent conductivity bias was applied to match the historical deep-water potential temperature–salinity relationship (○). Discounting the handful of profiles where the conductivity cell was obviously fouled, the residual main-thermocline water mass variations of ±0.01 pss are comparable to what has been seen by the Bermuda shipboard sampling program.

A two-axis tilt sensor integrated with the ACM and positioned within its electronics housing may be used to monitor mooring wire angles since the guide wheels force the profiler to align with the wire. Maximum tilts observed during the coastal deployment were ≲8° and were typically <2°; the largest tilts were at the bottom during episodes of strong horizontal flow, as predicted by mooring-response programs. The current meter measures orthogonal components of the flow, and so by using the tilt data, the relative velocity data may be rotated into true vertical and horizontal components. Also significant are the horizontal profiler motions relative to the ground as the instrument moves along the tilted mooring wire. Analysis for the flow in body coordinates (a coordinate system rotated into the plane of the local mooring wire slope) relates the ocean's horizontal velocity (u_o) to the measured relative velocities in body coordinates (u_r, w_r): $u_o = u_r \cos\theta - (w_r + d\ell/dt) \sin\theta$. Here, θ is the angle of the mooring wire from vertical and $d\ell/dt$ is the speed of the profiler along the wire. For small wire angles and weak ocean vertical velocity, the second and third terms in the expression (both of which depend strongly on the speed and direction of travel along the wire) tend to cancel, so that the measured velocity perpendicular to the mooring wire is a good estimate of the ocean's horizontal velocity. Insensitivity of the derived ocean current to direction of travel was confirmed in an analysis of 226 down–up profile pairs from the coastal deployment. For each available profile, the estimated speed of the horizontal ocean current (with no tilt corrections) between 1300- and 1400-m depth were averaged. The speeds sampled

on down-profiles were different from those sampled on the subsequent up-profiles by only 0.5 cm s^{-1} on average (up-profiles larger) with a standard deviation of 0.9 cm s^{-1}. This small difference between up- and down-going velocity estimates could be explained by a 1° misalignment of the current meter sensor sting relative to the vertical axis of the profiler body/guide wheels.

A similar analysis for the ocean's vertical velocity, w_o, yields $w_o = (w_r + dl/dt)\cos\theta + u_r \sin\theta$. Addition of a device to measure the instrument translation speed along the wire would facilitate estimation of the ocean's vertical velocity. However, assuming the pressure field is dominantly hydrostatic, the time rate of change of measured pressure provides an independent estimate of the profiler's vertical velocity, and in turn, an alternate estimate of w_o: $w_o = w_r \cos\theta + u_r \sin\theta + dZ(P)/dt$.

b. *Oceanographic sensors*

High-frequency noise levels of the MicroCTD instruments deployed on Moored Profilers appear consistent with the manufacturer's specifications. The standard deviations of high-passed (15-s cutoff period) temperature, conductivity, and pressure data from the coastal (Bermuda) deployment were 0.7 (0.5) m°C, 0.001 (0.0015) mmho, and 0.1 (0.2) db, respectively. On occasion, seaweed or some other material appeared to impact the conductivity sensors and greatly increase high-frequency noise (as well as temporarily shift the sensor calibration, see below).

Laboratory calibration data obtained before and after profiler deployments shed light on the stability of the temperature and pressure sensors. Owing to frequent modifications and upgrades to the instrumentation between deployments, we do not as yet have a long time-history of any one sensor. Short-term stability appears good. For example, the postrecovery temperature sensor calibration of the CTD instrument used on the fall 1997 coastal deployment was within 3 m°C^{-1} of that obtained prior to the deployment over the temperature range 1°–30°C. Pre- and postdeployment laboratory pressure calibrations typically agree to better than 5 db over the range 0–6000 db with the difference largely described by a bias change. It is our intent to monitor the sensors through repeated laboratory calibrations over extended time periods once the instrument design is stabilized.

Stability of the CTD pressure sensors were also assessed using in situ observations. On both the coastal and Bermuda deployments, the instruments were instructed to profile to the bottom stop (which was positioned within 100 m of the anchor). Thus, change in the observed maximum pressure sampled on each profile may be interpreted as sensor drift, as any mooring blowdown in strong flow causes little depth change of the bottom stop. Maximum observed pressure decreased over the first 10–20 profiling cycles in these two deployments, then remained stable (±1 db) for the balance of the deployments. During the coastal deployment

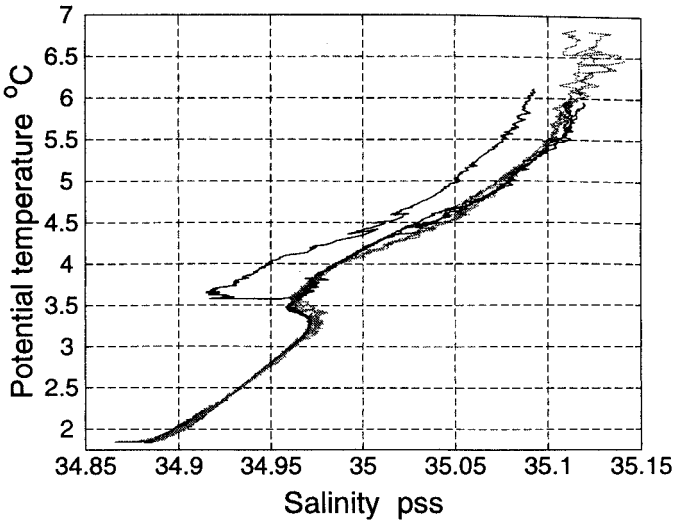

FIG. 7. Potential temperature–salinity curves from selected profiles from the beginning (black) and end (gray) of the 1997 Bermuda deployment. A bias correction was applied to conductivity on each profile to match the historical deep-water potential temperature–salinity relationship. Also shown is an example of a profile where the conductivity sensor was fouled, probably by seaweed (notable by anomalously low-salinity values at potential temperatures warmer than about 3.5°C).

(maximum pressure = 1430 db), the pressure drifted a total of 6 db; the Bermuda data (maximum pressure = 4370 db) show a 6-db drift in the first two cycles, followed by an additional 5–6-db drift over the next 10 cycles. A comparable analysis of sensor drift using data at the top mooring stop is precluded by real top-stop depth changes associated with mooring motion. However, comparison of the engineering pressure sensor observations with those from the CTD suggest similar CTD pressure drift behavior with time at the lower pressures of the top stop. (Thus, the MicroCTD pressure sensor drift appears to be basically a bias error, correctable by monitoring pressure at the bottom-stop.) Analysis of more recent deployments of CTDs with upgraded pressure sensors show bottom-stop pressure drifts of less than 2 db.

Conductivity sensor behavior may be monitored with in situ data if the instrument profiles a segment of the water column having a stable deep water potential temperature–salinity relationship. The deep waters off Bermuda satisfy this requirement. Raw conductivity observations on deep isotherms fluctuated by ±0.01 mmho during the Bermuda deployment (Fig. 6) superimposed on a drift of comparable magnitude towards larger values with time. Time-dependent adjustment of the cell calibration to force the deep temperature–salinity data to agree with observations from the Bermuda Atlantic Time Series Station (BATS: Michaels and Knap 1996) is reasonably successful in producing valid salinity data at all depths (Fig. 7). Those profiles exhibiting highly anomalous salinity data at thermocline depth (Fig. 6) are obviously affected by cell fouling (e.g., Fig. 7). Because the cell appears to recover substantially after these

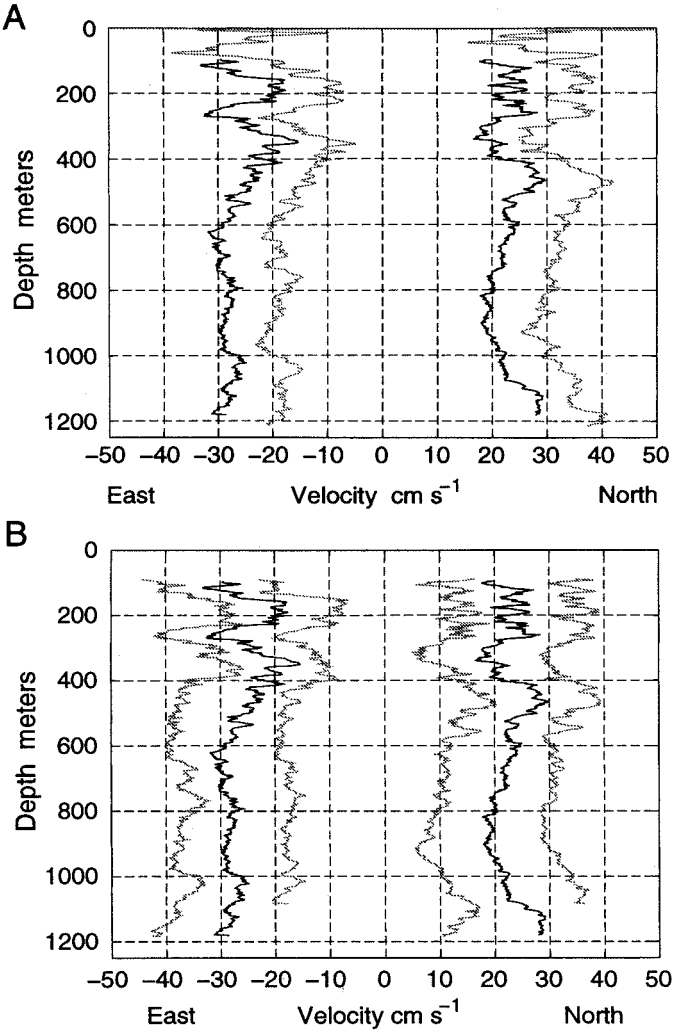

FIG. 8. (a) East and north components of ocean velocity observed on one vertical traverse by a Moored Profiler in May–June 1998 (black lines) with a nearly simultaneous profile obtained with an Expendable Current Profiler (XCP, gray line) deployed within 1 km of the mooring. Both profiles have been binned at 2-m vertical resolution. The (absolute) Moored Profiler components have been offset by −25 (east) and +25 (north) cm s^{-1} for clarity. The relative XCP components were referenced to the absolute profiler components by matching depth-averaged values and are plotted offset by +10 cm s^{-1} from their respective Moored Profiler components. (b) East and north components of ocean velocity simultaneously observed by three Moored Profilers spaced horizontally by approximately 500 m. The black curve is the same velocity profile shown in (a), similarly offset. The two companion velocity profiles (gray curves) have been offset from the first by −10 and +10 cm s^{-1} for clarity.

events, we believe seaweed or other material occasionally drapes over the cell (as opposed to something attaching and possibly growing on the cell; the cell was, in fact, visually clean on recovery.) Being in shallower water, an in situ check of the coastal deployment conductivity data is more problematic as real temperature–salinity variability cannot be ruled out. With a constant cell calibration derived to match reference salinity data obtained on mooring recovery, salinity on potential isotherms of about 800–1100-m depth exhibited variations ranging over 0.03 pss (discounting those handful of profiles where the cell was obviously fouled). These variations are slow in time (spanning multiple profiles), as might be expected from real ocean water mass change on the continental slope. The differences in salinity on isotherms between successive profiles have a standard deviation of only 0.002 pss. Ongoing trials offshore from Bermuda will further investigate longer-term conductivity sensor stability, exploiting the stable deep water properties there and the BATS observations as reference information.

Noise in the raw path-velocities of the ACM were estimated from high-pass-filtered time series (cutoff filter of 33-s period, where frequency spectra of the path-velocities flatten). When incident horizontal currents were less than about 10 cm s^{-1}, the standard deviation of the high-passed raw velocity data was 0.6–0.9 cm s^{-1}. This increased to 1.3–1.5 cm s^{-1} when incident currents approached 20 cm s^{-1}. The velocity noise is chiefly due to instrument vibrations associated with profiling along the irregular mooring wire; the high-frequency standard deviations drop to around 0.1 cm s^{-1} after the drive motor is shut down at the bottom stop. (The current meter collects data for a few minutes after the profiler hits the mooring stops.) Assuming the noise in each 2-Hz sample is independent and normally distributed, the standard error in 2-m-averaged velocity estimates is $\lesssim$0.6 cm s^{-1} and in 10-m averages is $\lesssim$0.3 cm s^{-1}. Bias error in the raw path-velocity data was quantified in the WHOI tow-tank facility and investigated using the in situ observations. (Unlike conventional instruments that vector average data in time, the profiler records raw data, allowing bias corrections during postrecovery processing.) These latter observations from the bottom stop (when all four channels should read the same velocity value if the instrument is aligned with the incident flow) hinted that one of the ACM channels had a bias of approximately 3 cm s^{-1}, a factor of 2 larger than observed in the tow-tank. This is currently under investigation.

An experiment conducted in May–June 1998 on the continental slope east of Virginia provided an opportunity to compare velocity profiles from the Moored Profiler and an Expendable Current Profiler (XCP). Three profiler moorings were deployed in this experiment, configured much like the 1997 coastal trial described above. The profilers were synchronized to initiate a cycle from the bottom stop (1100–1200 m) to the top stop (~100 m) and back every 3 h. The XCP was launched within 1 km of these moorings when the profilers were midway between their top and bottom stops. Good correspondence is seen between the two independent measurements of ocean velocity (Fig. 8a). Depth offsets of individual velocity features may be due to error in the XCP fall-rate prescription. Comparison of the simultaneous Moored Profiler velocity data from the three instruments (deployed in a triangular array with about 500 m between moorings) (Fig. 8b) suggests that much of the remaining profiler–XCP differences

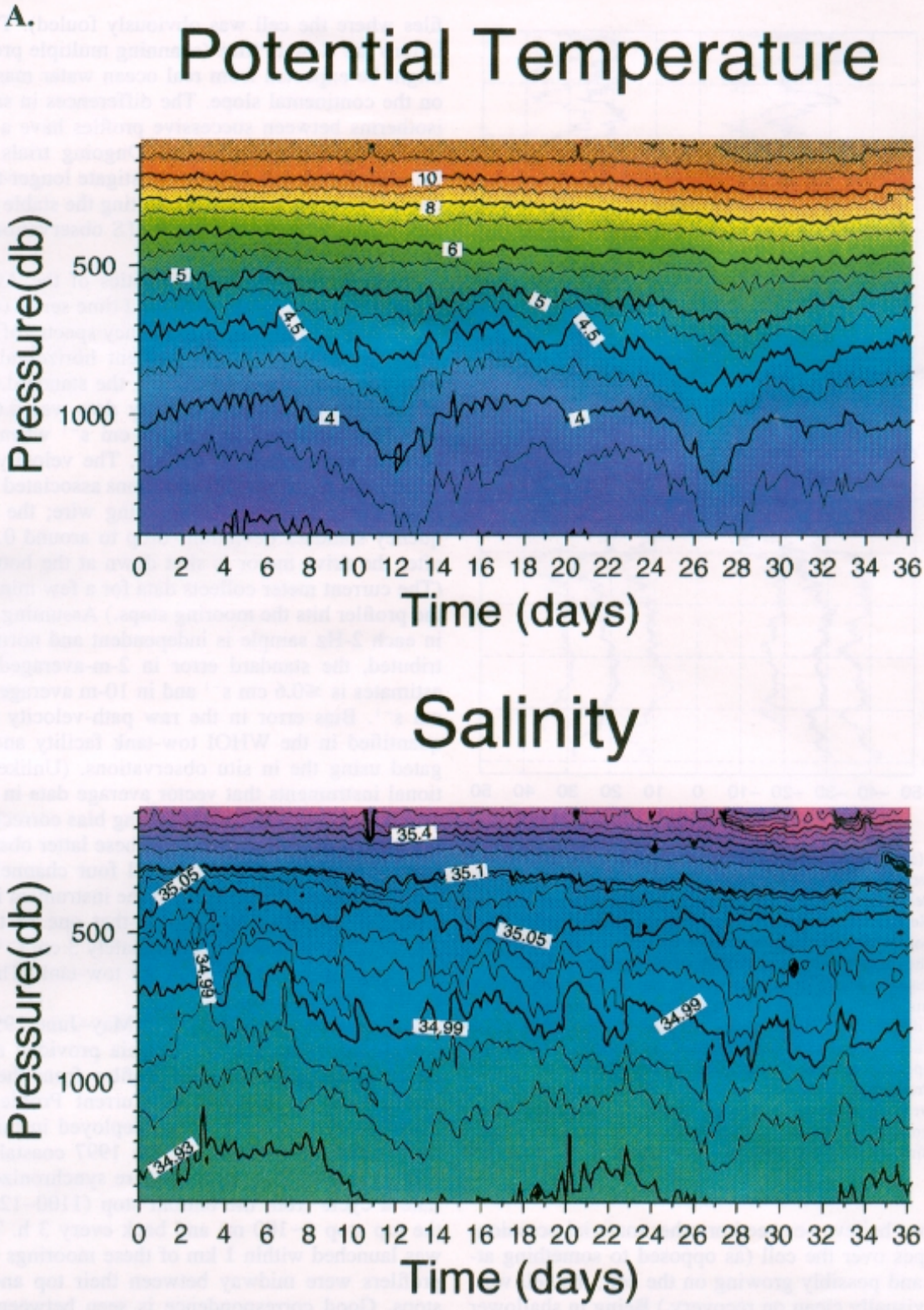

Fig. 9. Depth-time contoured data from the Moored Profiler deployed on the New England continental slope. (a) Temperature and salinity data and (b) the east and north velocity components. For this display, the data were regridded to 20 db and 4 h prior to contouring.

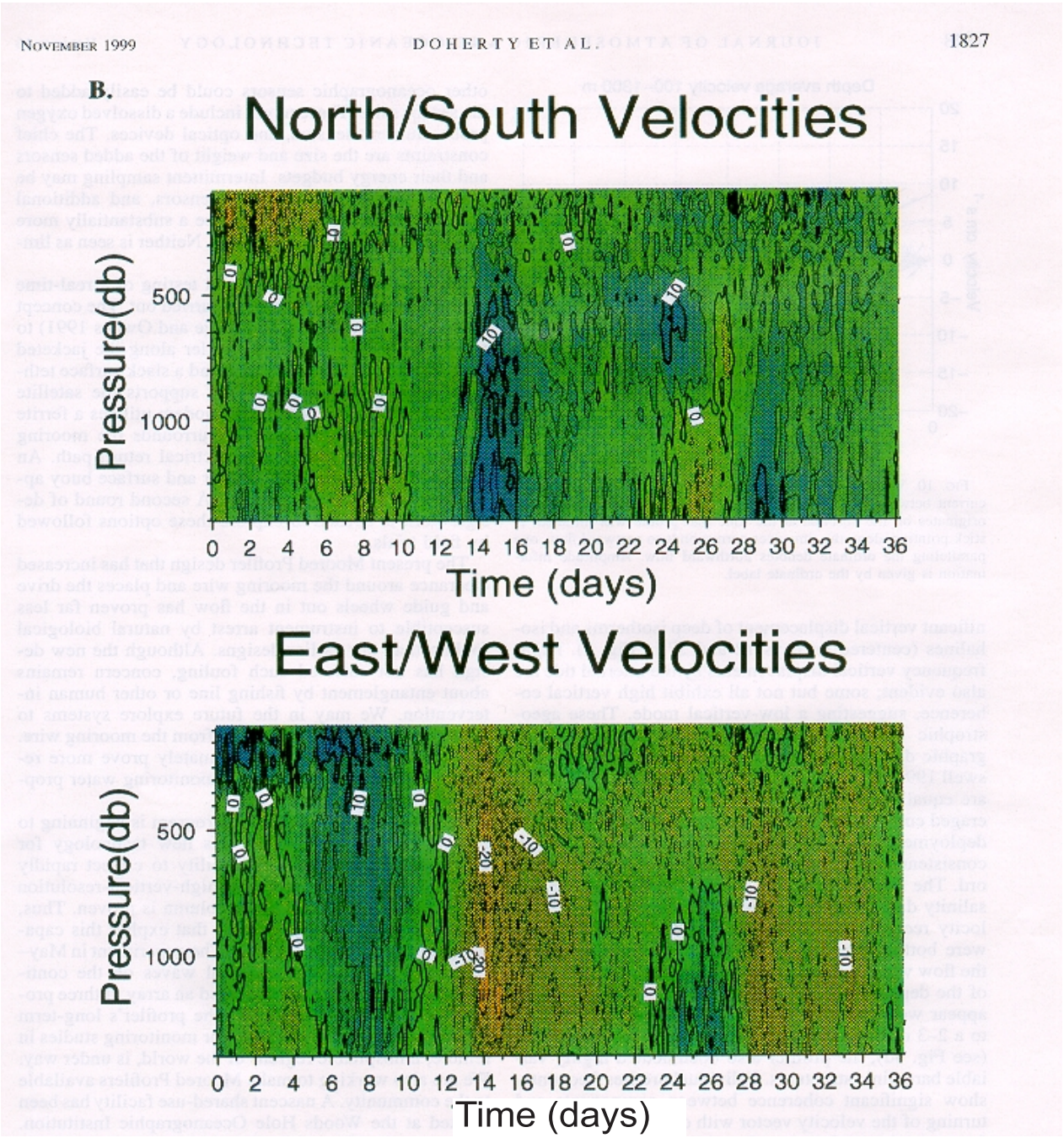

Fig. 9. (Continued)

may be real. A detailed analysis of the spring 1998 data is under way.

The 1997 time series data from the continental slope evince the exciting science that is possible with this new instrument. The general stratification at this time had temperature and salinity both decreasing with depth. On long time scales, the upper waters appeared to warm and increase in salinity (Fig. 9a), probably the result of onshore advection of the shelf-break front. Two mesoscale events were sampled by the mooring that caused sig-

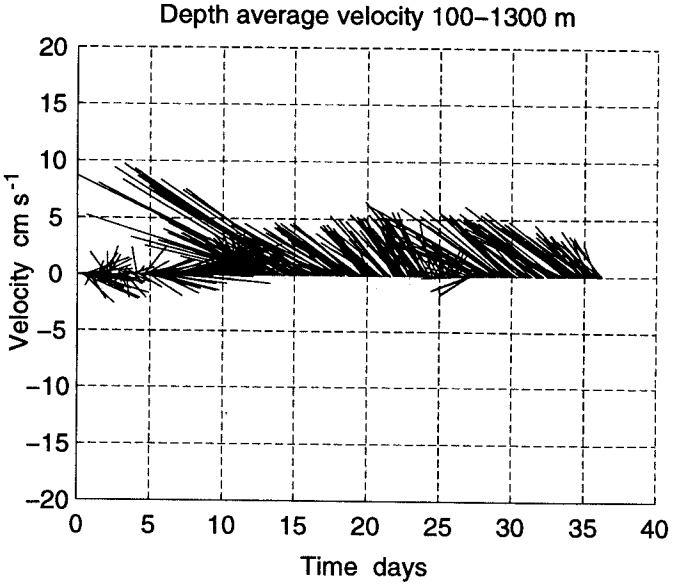

FIG. 10. Vector time series plot of the vertically averaged ocean current between 200- and 1300-m depth. A vector for each profile originates on the abscissa at the time that profile was initiated. A stick pointing along the time axes corresponds to eastward flow, one paralleling the ordinate denotes northward flow. Amplitude information is given by the ordinate label.

nificant vertical displacement of deep isotherms and isohalines (centered on days 12 and 27 in Fig. 9). High-frequency vertical displacements by the internal tide are also evident; some but not all exhibit high vertical coherence, suggesting a low-vertical mode. These ageostrophic motions potentially alias traditional hydrographic data and geostrophic transport estimates (Chiswell 1994). The accompanying horizontal velocity data are equally rich in temporal variability. The depth-averaged current was directed to the northwest during this deployment (Fig. 10), the northward component being consistent with the warming trend seen through the record. The mesoscale events seen in the temperature and salinity data are also evident in the depth-averaged velocity record. As seen in Fig. 9b, these flow features were bottom-intensified. At other times in the record, the flow was strongest at the surface (e.g., the first week of the deployment). At higher frequency, tidal currents appear well resolved by the 2-h sampling. In addition to a 2–3 cm s^{-1} peak-to-peak amplitude barotropic tide (see Fig. 4d), the profiler also documented highly variable baroclinic structures. Individual profiles frequently show significant coherence between components and turning of the velocity vector with depth typical of low-frequency internal waves. Ongoing analysis will investigate relationships between the barotropic and baroclinic tides and other internal waves, and the nature of these baroclinic mesoscale flow features.

4. Discussion and future plans

The Moored Profiler has thus far been equipped with a CTD and an ACM. Given its flexible control system, other oceanographic sensors could be easily added to the sensor suite. These might include a dissolved oxygen probe, nutrient sensors, and optical devices. The chief constraints are the size and weight of the added sensors and their energy budgets. Intermittent sampling may be required for "power-hungry" sensors, and additional buoyancy may be need to balance a substantially more massive instrumentation payload. Neither is seen as limiting.

Preliminary design and partial testing of a real-time data telemetry system has been carried out. The concept utilizes an inductive modem (Frye and Owens 1991) to relay information from the profiler along the jacketed (hence insulated) mooring wire and a slack surface tether to a small surface buoy that supports the satellite communication hardware. The modem utilizes a ferrite core fitted to the profiler that surrounds the mooring wire. Seawater provides the electrical return path. An acoustic link between the profiler and surface buoy appears to be a viable alternative. A second round of design work is needed to explore these options followed by field trials.

The present Moored Profiler design that has increased clearance around the mooring wire and places the drive and guide wheels out in the flow has proven far less susceptible to instrument arrest by natural biological fouling than our earlier designs. Although the new design has not suffered such fouling, concern remains about entanglement by fishing line or other human intervention. We may in the future explore systems to clear these types of obstructions from the mooring wire. Profiling free vehicles may ultimately prove more reliable than moored systems for monitoring water properties in heavily fished regions.

The Moored Profiler testing program is beginning to demonstrate the promise of this new technology for oceanographic research. The ability to collect rapidly sampled time series data at high-vertical-resolution nearly spanning the full water column is proven. Thus, limited-duration process studies that exploit this capability are immediately possible. The experiment in May–June 1998 investigating internal waves on the continental slope successfully deployed an array of three profilers in this mode. Testing of the profiler's long-term behavior, a capability required for monitoring studies in remote, inhospitable regions of the world, is under way. We are also working to make Moored Profilers available to the community. A nascent shared-use facility has been created at the Woods Hole Oceanographic Institution. Moreover, the Moored Profiler technology has been licensed to McLane Research Laboratories, Inc., of Falmouth, Massachusetts, which anticipates commercial release of the system when development is complete.

Acknowledgments. Initial development and testing of the Moored Profiler was supported by the Ocean Technology Program of the National Science Foundation and the WHOI Director's discretionary fund. Additional de-

velopment and testing have been funded by the Office of Naval Research, and the NOAA–University Consortium program. We greatly appreciate this support and the sustained confidence of our program managers through our lengthy and at times trying development program. We wish to also acknowledge the technical support to the project provided by M. Cook, K. Fairhurst, T. Hammar, A. Hinton, E. Hobart, J. Kemp, N. McPhee, E. Montgomery, and G. Packard, and thanks to E. Kunze for providing the XCP data.

REFERENCES

Chiswell, S. M., 1994: Vertical structure of the baroclinic tides in the central North Pacific Subtropical Gyre. *J. Phys. Oceanogr.*, **24,** 2032–2039.

Denman, K. L., H. J. Freeland, and J. F. Garrett, 1992: Climate change in the subarctic Pacific Ocean, Part 1: Atmospheric and oceanic evidence. *North Pacific Marine Science Organization (PICES), PICES Scientific Workshop,* Seattle, WA, 1–6.

Dickey, T., D. Frye, H. Jannasch, E. Boyle, and A. Knap, 1997: Bermuda sensor system testbed. *Sea Tech.*, **38** (4), 81–86.

Eckert, A. C., J. H. Morrison, G. B. White, and E. W. Geller, 1989: The autonomous ocean profiler: A current driven oceanographic sensor platform. *IEEE J. Oceanic Eng.*, **14,** 195–202.

Eriksen, C. C., J. M. Dahlen, and J. T. Shillingford Jr., 1982: An upper ocean moored current and density profiler applied to winter conditions near Bermuda. *J. Geophys. Res.*, **87,** 7879–7902.

Fowler, G. A., J. M. Hamilton, B. D. Beanlands, D. J. Belliveau, and A. R. Furlong, 1997: A wave-powered profiler for long-term monitoring. *Proc. Oceans '97 MTS IEEE Conf.,* Halifax, NS, Canada, 225–229.

Freeland, H. J., K. L. Denman, C. S. Wong, F. Whitney, and R. Jacques, 1997: Evidence of change in the N.E. Pacific Ocean. *Deep-Sea Res.*, **44,** 2117–2129.

Frye, D. E., and W. B. Owens, 1991: Recent developments in ocean data telemetry at Woods Hole Oceanographic Institution. *IEEE J. Oceanic Eng.*, **16,** 350–359.

Hayes, S. P., R. Ripa, and L. J. Mangum, 1985: On resolving vertical modes with observational data. *J. Geophys. Res.*, **90,** 7227–7234.

——, L. J. Mangum, J. Picaut, A. Sumi, and K. Takeuchi, 1991: TOGA-TAO: A moored array for real-time measurements in the tropical Pacific Ocean. *Bull. Amer. Meteor. Soc.*, **72,** 339–347.

Joyce, T. M., and P. Robbins, 1996: The long-term hydrographic record at Bermuda. *J. Climate,* **9,** 3121–3131.

Karl, D. M., and A. F. Michaels, 1996: Ocean time-series: Results from the Hawaii and Bermuda research programs. *Deep-Sea Res.*, **43,** 127–686.

Lazier, J. R., 1980: Oceanographic conditions at O.W.S. *Bravo,* 1964–1974. *Atmos.–Ocean,* **18,** 227–238.

Michaels, A. F., and A. H. Knap, 1996: Overview of the U.S. JGOFS Bermuda Atlantic Time-Series study and the Hydrostation S program. *Deep-Sea Res.*, **43,** 157–198.

Østerhus, S., T. Gammerlsrød, and R. Hogstad, 1996: Ocean weather ship station M (66°N, 2°E): The longest homogeneous time series from the deep ocean. *Int. WOCE Newsl.*, **24,** 31–33.

Provost, C., and M. du Chaffaut, 1996: Yoyo Profiler: An autonomous multi-sensor. *Sea Tech.*, **37** (10), 39–45.

Savage, G., and J. Hersey, 1968: Project Seaspider report. WHOI Tech. Rep. WHOI-68-42, 142 pp. [NTIS AD-673 956/XA3.]

Talley, L., 1996: North Atlantic circulation and variability. *Physica D,* **98,** 625–646.

——, and M. E. Raymer, 1982: Eighteen degree water variability. *J. Mar. Res.*, **40** (Suppl.), 757–775.

Van Leer, J., W. Düing, R. Erath, E. Kennelly, and A. Speidel, 1974: The Cyclesonde: An unattended vertical profiler for scaler and vector quantities in the upper ocean. *Deep-Sea Res.*, **21,** 385–400.